Blood Detection in Wireless Capsule Endoscope Images based on Salient Superpixels

Dimitris K. Iakovidis, *Senior Member, IEEE*, Dimitris Chatzis, Panos Chrysanthopoulos, and Anastasios Koulaouzidis

***Abstract*—Wireless capsule endoscopy (WCE) enables screening of the gastrointestinal (GI) tract with a miniature, optical endoscope packed within a small swallowable capsule, wirelessly transmitting color images. In this paper we propose a novel method for automatic blood detection in contemporary WCE images. Blood is an alarming indication for the presence of pathologies requiring further treatment. The proposed method is based on a new definition of superpixel saliency. The saliency of superpixels is assessed upon their color, enabling the identification of image regions that are likely to contain blood. The blood patterns are recognized by their color features using a supervised learning machine. Experiments performed on a public dataset using automatically selected first-order statistical features from various color components indicate that the proposed method outperforms state-of-the-art methods.**

I. Introduction

Wireless capsule endoscopy (WCE) has evolved from disruptive technological achievement at the dawn of the millennium to a well-established and trusted method for diagnostic digestive endoscopy [1]. National and international societies propose that WCE is incorporated in the algorithm of investigation of obscure gastrointestinal bleeding (OGIB) [2, 3]. It is noteworthy that the aetiology of the bleeding remains unknown after upper and lower digestive endoscopy in approximately 10% to 20% of cases [3]. Therefore, OGIB is the most frequent accepted indication for WCE examination once upper and lower endoscopy have failed to identify the bleeding source [2]. Recently, there is a renewed interest in the use of WCE at the emergency clinical setting as a game-changing strategy that could lead to a better use of endoscopic resources and rationalization of critical care bed occupancy [4].

Nevertheless, instant blood detection and alarm of the treating team is required in order to achieve a timely and appropriate intervention [5]. The former, even with the use of the real-time viewer capacity, requires staff input which greatly diminishes the chance for optimising WCE potential in the acute clinical setting. Furthermore, over the last few years, the need for automatic abnormality detection and diagnosis has become one of the 'holy grail' requirements for WCE reading software development [6].

Angiectasias, abnormal dilatation of small blood vessels at the mucosa layer of the gut, are –by far– the commoner small-bowel finding in patients investigated for OGIB [1, 3]. Therefore, automatic detection of such type of lesions and intraluminal blood is necessary for further progress.

In this paper, we propose a novel method for blood detection in contemporary WCE images, based on a new definition of salient superpixels. Superpixels are perceptually meaningful atomic, spatially coherent regions within an image that can be obtained by image segmentation, and replace the rigid structure of the pixel grid. Salient superpixels are those that are more interesting than others. Considering the importance of color in the endoscopic diagnosis of digestive tract diseases [7], particularly in blood detection [6], superpixel saliency is assessed with respect to the color content of the WCE images.

The rest of this paper is organized in five sections. Section II reviews the previous work related to blood detection in WCE images. The concept of salient superpixels is introduced in section III, and its application for blood detection is described in section IV. The results of the experiments performed in comparison with a state-of-the-art blood detection method are presented and discussed in section V. The last section summarizes the contributions and the conclusions of this study.

II. Previous Work

Blood detection is one of the first challenges that have been investigated in the context of WCE image analysis [8]. Blood has a distinct red hue, which makes evident why the majority of the blood detection methods have been based on color features [6]. In this context Sainju et al [9] proposed a supervised blood detection method based on statistical features derived from the first order *RGB* color histogram probability of segmented image regions. A multilayer neural network classifier is trained with regions segmented by a semi-automatic region growing algorithm that is initialized with manually selected seed pixels.

Fu et al [10] proposed a method based on Simple Linear Iterative Clustering (SLIC) algorithm for superpixel segmentation of WCE images. Each superpixel is represented by vectors composed of the following color features:

$$F_1 = \frac{R(i)}{G(i)},\ F_2 = \frac{R(i)}{B(i)},\ F_3 = \frac{R(i)}{R(i)+G(i)+B(i)} \qquad (1)$$

*Research supported by the special account for research grants of the Technological Educational Institute of Central Greece (Central Greece University of Applied Sciences).

D.K. Iakovidis, is with the Department of Computer Engineering, Technological Educational Institute of Central Greece, 35100 Lamia, Greece (phone: +30-22310-60159, e-mail: dimitris.iakovidis@ieee.org).

D. Chatzis and P. Chrysanthopoulos are with the Department of Computer Science and Biomedical Informatics of the University of Thessaly, 35100, Lamia, Greece.

A. Koulaouzidis is with The Royal Infirmary of Edinburgh, Endoscopy Unit, Edinburgh, 51 Little France Crescent, Old Dalkeith Road, Edinburgh EH16 4SA, UK.

978-1-4244-9270-1/15/$31.00 ©2015 EU

where $R(i)$, $G(i)$, $B(i)$ are the mean values of the quantities of red, green and blue components of the pixels belonging at the i^{th} superpixel. Blood detection is performed via classification of the feature vectors into two classes corresponding to blood and normal patterns, by a Support Vector Machine (SVM).

A color-based abnormality detection method has been proposed by Iakovidis and Koulaouzidis [11, 12]. This method is capable of detecting several abnormalities including intraluminal bleeding and angioectasias. Initially, it automatically detects salient pixels based on their color. This is achieved by application of the interest point detection algorithm of Speeded-Up Robust Feature (SURF) [13] extraction method on color component *a* of the WCE images, which are represented in CIE-*Lab* color space [14]. For each salient pixel a feature vector (descriptor) is composed. The vector is composed of the *L*, *a*, *b* values of the salient pixel and the minimum and maximum *L*, *a*, *b* values of the pixels lying within a square neighborhood centered at the salient pixel. A significant finding of that study was that salient pixels were detected in all abnormalities of the dataset.

In this paper we enhance the superpixel-based blood detection approach of Fu et al [10] by a) co-evaluating the color saliency of the superpixels identified in the WCE images, and b) extracting more discriminative feature vectors for blood detection. Furthermore we provide a new definition of superpixel saliency, which unlike the one proposed in [15], takes into account the saliency of the pixels contained within the superpixels. This is important in cases where blood spots are smaller than the area of a superpixel.

III. Salient Superpixels

A. Superpixel segmentation

SLIC [16] is an adaptation of the well-known *k*-means algorithm for clustering pixels [17]. The resulting clusters of pixels are the so-called superpixels. Each pixel of an image *I* is represented by a five-dimensional feature vector composed of the values of the *L*, *a*, *b* color components and the pixel coordinates (*x*, *y*). The only parameter in SLIC algorithm is *k,* i.e., the number of superpixels in which the image will be segmented. The clustering procedure begins by initializing *k*-means with *k* feature vectors as cluster centers. These vectors are estimated from seed locations corresponding to the lowest gradient position in a 3×3 neighborhood of pixels sampled on a regular grid, spaced *S* pixels apart, where $S = \sqrt{N/k}$, and *N* is the number of pixels in *I*.

The algorithm proceeds by evaluating the distances between the feature vector extracted from each pixel and the cluster centers. SLIC differs from conventional *k*-means in that the number of distance calculations in the optimization is reduced. This is achieved by limiting the search area to a region proportional to the superpixel size. As a result the complexity is linear to the number of pixels and independent to the number of superpixels. The distance metric used is

$$D = \sqrt{d_c^2 + \left(\frac{d_s^2}{S}\right)^2 m^2} \tag{2}$$

where d_c is the distance between (*L*, *a*, *b*) vectors, d_s is the distance between (*x*, *y*) vectors, and *m* is a variable that controls the compactness of the superpixels.

B. Salient superpixel detection

The concept of salient pixels can be extended to the level of superpixels by exploiting a superpixel segmentation and a salient pixel detector.

Definition 1: Let *I* be an image segmented into a set *P* of *k* superpixels P_i such that

$$P = \{P_i \subseteq I, i = 1,...,k\},\ I = \bigcup_{i=1}^{k} P_i \tag{3}$$

and $P_i \cap P_j = \varnothing, \forall j \neq i, i = 1,...,k, j = 1,...,k$.

Given a set

$$\Pi = \{p_l \in I, l = 1,...,n\} \tag{4}$$

of *n* salient pixels p_l detected in *I*, a salient superpixel is defined as a member of

$$P' = \{P_i : \exists p_l \in P_i, i = 1,...,k, l = 1,...,n\} \tag{5}$$

where $P' \subseteq P$.

Based on this definition, the proposed salient superpixel detection involves in three steps: a) superpixel segmentation; b) salient pixel detection; and c) selection of a subset of superpixels containing at least one salient pixel.

IV. Blood Detection

The proposed blood detection method begins with the detection of salient superpixels in a WCE image, as described in section III. Salient pixel detection is performed using the salient pixel detector proposed in our previous works [11, 12], due to its effectiveness in WCE images. Figure 1 illustrates the salient superpixel detection process on representative images of intraluminal bleeding and of an angioectasia. It can be noticed that at least one superpixel per image corresponds to a (red) blood area.

Each salient superpixel is represented by a set of first order statistical color features extracted from *RGB* and other color spaces, where chromatic components are approximately decorrelated. These include the perceptually uniform CIE-*Lab* (or $L^*a^*b^*$) and the perceptual HSV color spaces, which can be derived from *RGB* with a non-linear transformation [14]. The components of CIE-*Lab*, represent lightness (*L*), the quantity of red (a>0) or the quantity of green (-a>0), the quantity of yellow (b>0) or the quantity of blue (-b>0). The components of HSV, represent hue (*H*), color saturation (*S*) and the value (*V*) of its lightness. In this paper the optimal feature subset selection process is determined experimentally, by application of feature selection algorithms, as described in section IV.

The blood pattern recognition task can be implemented by a supervised learning machine. In this work, we applied the non-linear, Radial Basis Function (RBF) SVM classifier [17], because it is well-known for its learning capacity and has exhibited a better performance than others in the related previous studies [10, 11, 12].

V. Experimental Evaluation

The experiments performed in this study aim to the selection of the best performing feature sets for blood

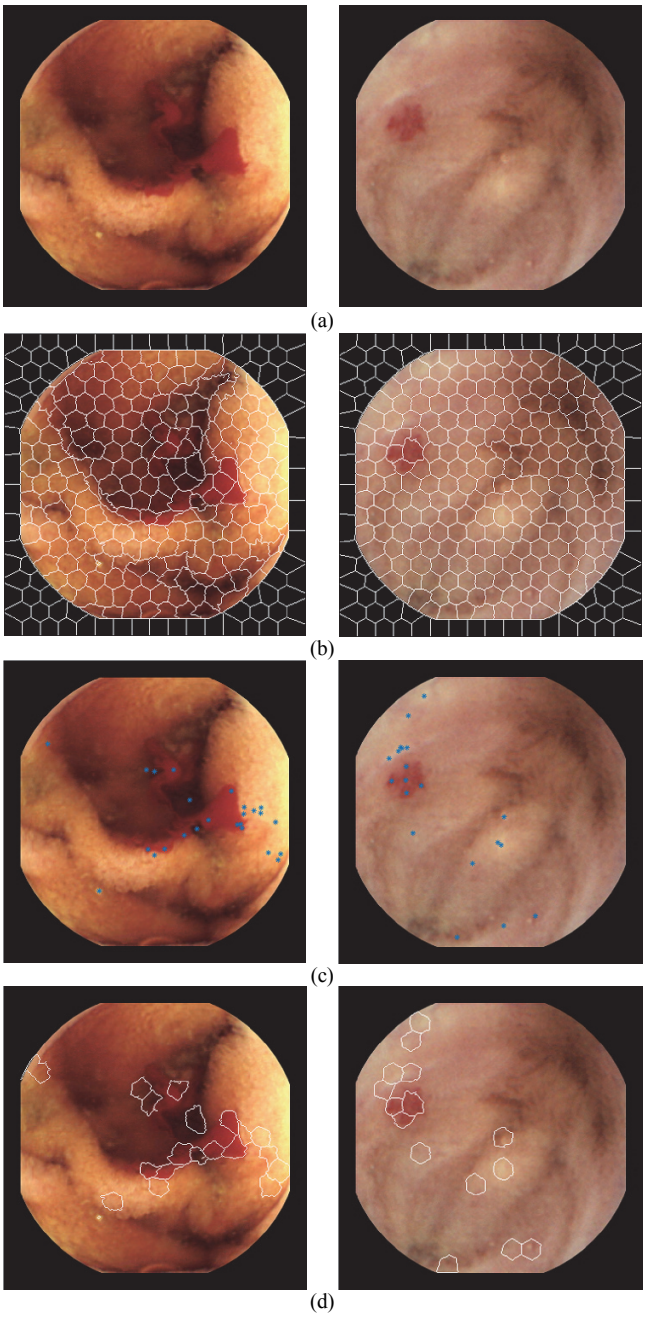

Figure 1. Salient superpixel detection in WCE images of intraluminal bleeding (left) and of an angioectasia (right). (a) Original images, (b) Segmented images using superpixel segmentation, (c) Detected salient pixels, (d) Detected salient superpixels.

detection in WCE images. The dataset used has been acquired with a MiroCam® (IntroMedic® Co., Seoul, South Korea) capsule endoscope, with a resolution of 320×320 pixels. It comprises a representative set of WCE images obtained from a total of 252 WCE procedures. A detailed description of this dataset is provided in [11, 12] and it is publicly available through our online WCE database KID[1] [6]. All images in this dataset are accompanied by ground truth graphic annotations performed manually by experts using the Ratsnake annotation tool [18]. Blood detection performance was assessed on the images of intraluminal bleeding and angioectasias, as well as on the normal images (without visible abnormalities) of the dataset. In order to account for more realistic conditions the normal images included bubbles and/or luminal debris or opaque luminal fluid.

The color features extracted from each superpixel include statistical (central) moments of up to 3rd order, estimated from color components $X=\{R, G, B, L, a, b, H, S, V, F_1, F_2, F_3\}$, where F_1, F_2 and F_3 are defined by Eq.(1). Optimal feature subsets for superpixel representation have been obtained with the application of feature selection and ranking algorithms that are based on different optimality conditions. These include [19]: a) Correlation-based Feature Selection (CFS), which selects a subset of attributes by considering the individual predictive ability of each feature along with the degree of redundancy between them; b) feature ranking based on the Information Gain (IG), the Gain Ratio (GR), and the chi-squared statistic (χ^2) with respect to the class; and c) Recursive Feature Elimination (RFE), which is a feature selection algorithm embedded in the SVM classification scheme. In all cases subsets of the ranked features of increasing cardinality, i.e., subsets composed of the first one, two, three features etc, formed feature vectors, which were subsequently classified by the SVM. The feature extraction methods were implemented in MATLAB, using the superpixel segmentation algorithm provided by Achanta et al [16], and the feature selection algorithms of WEKA data mining software [20]. The parameter ranges investigated by grid search include $k\in[200, 400]$, SURF threshold $t\in[100, 1000]$, SVM cost parameter $c\in[0.001, 1000]$ and RBF $\sigma\in[0.01, 1]$.

In order to minimize the bias in the selection of the training and test sets, repetitive classification experiments were carried out using the 10-fold cross validation strategy. The classification accuracy was assessed by the mean area under the receiver operating characteristic (ROC) curve (AUC), as it represents an intuitive performance measure even if the datasets have imbalanced class distributions [21]. The average sensitivity and specificity are also provided for reference with respect to the related works. For comparison purposes we have assessed the classification performance obtained using: a) the means of each *RGB*, CIE-*Lab* and *HSV* color space components, as a baseline approach; b) normalized histograms h_X, with 2^i bins, $i=1,\ldots,128$ per color component X; c) the method of Fu et al [10]; and d) our state-of-the-art abnormality detection method [11], which is now applied only for blood detection.

The best average results obtained with the different methods are summarized in Table I. The feature selection process showed that only three features are sufficient for blood discrimination. No increase in AUC was observed by increasing the dimension of the feature vectors with lower ranked features. The selected features include only first and second order moments (mean μ_X, and standard deviation σ_X). IG and χ^2 –based ranking gave the same feature subsets in the top-three positions. Best classification performance was achieved with the feature subset selected by the CFS method.

The baseline approach resulted in approximately the same classification performance for all color spaces considered (indicatively Table I includes the performance of CIE-*Lab*

[1] http://is-innovation.eu/kid/

means). The best performing histograms were those of the *a* CIE-*Lab* component (h_a) using 32 bins. Although the AUC obtained by the histogram features is quite high, its large dimensionality leads to a more complex classification stage than the (3-dimensional) feature vector obtained from the CFS algorithm.

Table I shows also that the CFS-based feature subset outperforms both the state-of-the-art methods of Fu et al [10] and Iakovidis and Koulaouzidis [11]. In order to assess the effect of color saliency in the feature extraction process, the method of Fu et al was tested both in its original version [10], using features extracted from all superpixels (29,440) and using features extracted only from salient superpixels (3,501). In the latter case the mean AUC obtained was 0.86±0.05, i.e., approximately the same to the former (Table I). Therefore, the use of salient superpixels can be used for a less complex feature extraction process requiring 740% less feature vector computations.

TABLE I. SUMMARY OF BLOOD DETECTION RESULTS.

Method (feature subset)	Sens.	Spec.	AUC
CFS (μ_a , σ_a , μ_S)	**0.96±0.00**	**0.91±0.03**	**0.94±0.01**
IG, χ^2 (μ_a , μ_{F1} , μ_{F3})	0.95±0.00	0.85±0.03	0.90±0.02
GR (μ_a , μ_S , μ_{F1})	0.95±0.01	0.86±0.05	0.90±0.03
RFE (σ_a , μ_H , σ_S)	0.93±0.00	0.77±0.11	0.85±0.05
Baseline (μ_L , μ_a , μ_b)	0.94±0.01	0.82±0.10	0.88±0.04
Histogram 32 bins (h_a)	0.95±0.00	0.88±0.07	0.92±0.04
Fu et al [10] (μ_{F1} , μ_{F2} , μ_{F3})	0.88±0.01	0.84±0.06	0.86±0.06
Iakovidis & Koulaouzidis [11]	0.99±0.00	0.78±0.08	0.89±0.04

VI. CONCLUSION

A novel blood detection method for WCE, based on superpixel segmentation and color saliency, is presented. The experimentation performed indicates that proposed method is more effective than its state-of-the-art predecessors [10, 11], and in the case of [10] also more efficient.

In [10] the average results reported are higher (accuracy 0.95, sensitivity 0.99, and specificity 0.94) than the ones obtained in our study for the same method (accuracy 0.86, sensitivity 0.88, specificity 0.84). This is confirms that the results reported in different studies for WCE are highly dependent on the datasets [6]. The dataset used in [10] originates from the public database of Given Imaging [22]; however, the experiments are not fully reproducible because the video clips used are not specified, the randomly selected subset of the video frames used is not provided, and the image annotations used are also not provided. The dataset used in our study is also publicly available, but the specific images and annotations are provided; thus enabling comparisons with both current and future methodologies.

Future work includes large scale experimentation using full WCE videos, further investigation of color saliency for WCE images, and enhancement of the proposed approach so that it can be more reliably used for recognition of other abnormalities, such as ulcers and polyps.

REFERENCES

[1] A. Koulaouzidis, E. Rondonotti, and A. Karargyris, "Small-bowel capsule endoscopy: a ten-point contemporary review," *World journal of gastroenterology: WJG*, vol. 19, no. 24, p. 3726, 2013.

[2] M. Pennazio, C. Spada, R. Eliakim, M. Keuchel, A. May, C. J. Mulder, E. Rondonotti, S. N. Adler, J. Albert, P. Baltes *et al.*, "Small-bowel capsule endoscopy and device-assisted enteroscopy for diagnosis and treatment of small-bowel disorders: European society of gastrointestinal endoscopy (esge) clinical guideline," *Endoscopy*, vol. 47, no. 04, pp. 352–386, 2015.

[3] E. Rondonotti, A. Koulaouzidis, S. Paggi, F. Radaelli, and M. Pennazio, "Obscure gastrointestinal bleeding and iron-deficiency anemia—where does capsule endoscopy fit?" *Techniques in Gastrointestinal Endoscopy*.

[4] M. Peláez-Luna, "Emergency video capsule endoscopy: A game-changing strategy? toward a better use of endoscopic resources," *Gastrointestinal endoscopy*, vol. 81, no. 4, pp. 896–897, 2015.

[5] C. Schlag, C. Menzel, S. Nennstiel, B. Neu, V. Phillip, T. Schuster, R. M. Schmid, and S. von Delius, "Emergency video capsule endoscopy in patients with acute severe gi bleeding and negative upper endoscopy results," *Gastrointestinal endoscopy*, 2014.

[6] D. K. Iakovidis and A. Koulaouzidis, "Software for enhanced video capsule endoscopy: challenges for essential progress," *Nature Reviews Gastroenterology & Hepatology*, vol. 12, no. 3, pp. 172–186, 2015.

[7] M. Tanaka, Y. Kidoh, M. Kamei, T. Terasaki, A. Watanabe, T. Sakamoto, and M. Fujimaki, "A new instrument for measurement of gastrointestinal mucosal color," *Digestive Endoscopy*, vol. 8, no. 2, pp. 139–146, 1996.

[8] M. Boulougoura, E. Wadge, V. Kodogiannis, and H. S. Chowdrey, "Intelligent systems for computer-assisted clinical endoscopic image analysis," in *2nd IASTED Int. Conf. on Biomedical Engineering, Innsbruck, Austria*, 2004, pp. 405–408.

[9] S. Sainju, F. M. Bui, and K. A. Wahid, "Automated bleeding detection in capsule endoscopy videos using statistical features and region growing," *Journal of Medical Systems*, vol. 38, no. 4, pp. 1–11, 2014.

[10] Y. Fu, W. Zhang, M. Mandal, and M.-H. Meng, "Computer-aided bleeding detection in wce video," *IEEE Journal of Biomedical and Health Informatics*, vol. 18, no. 2, pp. 636–642, 2014.

[11] D. K. Iakovidis and A. Koulaouzidis, "Automatic lesion detection in capsule endoscopy based on color saliency: closer to an essential adjunct for reviewing software," *Gastrointestinal endoscopy*, vol. 80, no. 5, pp. 877–883, 2014.

[12] D. K. Iakovidis and A. Koulaouzidis, "Automatic lesion detection in wireless capsule endoscopy—a simple solution for a complex problem," in *Image Processing (ICIP), 2014 IEEE International Conference on*. IEEE, 2014, pp. 2236–2240.

[13] H. Bay, A. Ess, T. Tuytelaars, and L. Van Gool, "Speeded-up robust features (surf)," *Computer vision and image understanding*, vol. 110, no. 3, pp. 346–359, 2008.

[14] G. Wyszecki and W. S. Stiles, *Color science*. Wiley New York, 1982.

[15] S. Huang, W. Wang, and H. Zhang, "Retrieving images using saliency detection and graph matching," in *Image Processing (ICIP), 2014 IEEE International Conference on*. IEEE, 2014, pp. 3087–3091.

[16] R. Achanta, A. Shaji, K. Smith, A. Lucchi, P. Fua, and S. Susstrunk, "Slic superpixels compared to state-of-the-art superpixel methods," *Pattern Analysis and Machine Intelligence, IEEE Transactions on*, vol. 34, no. 11, pp. 2274–2282, 2012.

[17] S. Theodoridis and K. Koutroumbas, *Pattern Recognition*. Elsevier/Academic Press, 2008.

[18] D. Iakovidis, T. Goudas, C. Smailis, and I. Maglogiannis, "Ratsnake: A versatile image annotation tool with application to computer-aided diagnosis," *The Scientific World Journal*, vol. 2014, no. 286856, 2014.

[19] H. Liu and H. Motoda, *Computational methods of feature selection*. CRC Press, 2007.

[20] M. Hall, E. Frank, G. Holmes, B. Pfahringer, P. Reutemann, and I. H. Witten, "The weka data mining software: an update," *ACM SIGKDD explorations newsletter*, vol. 11, no. 1, pp. 10–18, 2009.

[21] T. Fawcett, "An introduction to roc analysis," *Pattern recognition letters*, vol. 27, no. 8, pp. 861–874, 2006.

[22] Capsuleendoscopy.org image atlas. Given Imaging. [Online]. Available: http://www.capsuleendoscopy.org/